Generation of Nucleophilic Character in the Cys25/His159 Ion Pair of Papain Involves Trp177 but Not Asp158[†]

Sheraz Gul,[‡,§,||] Syeed Hussain,[‡,||,⊥] Mark P. Thomas,[‡,∞] Marina Resmini,[@] Chandra S. Verma,[#] Emrys W. Thomas,[+] and Keith Brocklehurst*[,‡]

Laboratory of Structural and Mechanistic Enzymology, School of Biological and Chemical Sciences, Fogg Building, Queen Mary, University of London, Mile End Road, London E1 4NS, U.K., School of Biological and Chemical Sciences, Walter Bessant Building, Queen Mary, University of London, Mile End Road, London E1 4NS, U.K., Bioinformatics Institute, 30, Biopolis Way, #07-01 Matrix, Singapore 138671, and Department of Biological Sciences, University of Salford, The Crescent, Salford M5 4JW, U.K.

Received October 23, 2007; Revised Manuscript Received December 10, 2007

ABSTRACT: Studies on papain (EC 3.4.22.2), the most thoroughly investigated member of the cysteine proteinase superfamily, have contributed substantially to our understanding of the roles of noncovalent interactions in enzyme active center chemistry. Previously, we reported evidence that the long-held view that catalytic competence develops synchronously with formation of the catalytic site (Cys25)−S^-/(His159)−Im^+H ion pair is incorrect and that conformational rearrangement is necessary for each of the partners to play its role in catalysis. A decrease in the level of mutual solvation of the partners of the noncatalytic "intimate" ion pair should release the nucleophilic character of (Cys25)−S^- and allow association of (His159)−Im^+H with the leaving group of a substrate to provide its general acid-catalyzed elimination. Hypotheses by which this could be achieved involve electrostatic modulation of the ion pair and perturbation of its hydrophobic shielding from solvent by Trp177. The potential electrostatic modulator closest to the catalytic site is Asp158, the mutation of which to Ala substantially decreases catalytic activity. Here we report an investigation of these hypotheses by a combination of computer modeling and stopped-flow pH-dependent kinetic studies using a new series of cationic aminoalkyl 2-pyridyl disulfide time-dependent inhibitors as reactivity probes. These probes **2**−**4** ($n = 2-4$), which exist as equilibrium mixtures of H_3N^+-$[CH_2]_n$-S-S-2-pyridyl$^+$H and H_3N^+-$[CH_2]_n$-S-S-2-pyridyl which predominate in acidic and weakly alkaline media, respectively, were shown by modeling and kinetic analysis to bind with various degrees of effectiveness near Asp158 and in some cases also near Trp177. Kinetic analysis of the reactions of **2**−**4** and of the reaction of CH_3-$[CH_2]_2$-S-S-2-pyridyl$^+$H ⇌ CH_3-$[CH_2]_2$-S-S-2-pyridyl **1** and normal mode calculations lead to the conclusion that Asp158 is not involved in the generation of nucleophilic character in the ion pair and demonstrates a key role for Trp177.

Understanding the roles of noncovalent interactions both within the enzyme molecule and between enzyme and substrate or inhibitor is an important goal of the investigation of enzyme active center chemistry and catalytic mechanism, and studies on the papain family of cysteine proteinases (cysteine peptidases) continue to illuminate aspects of this goal. The cysteine proteinases are widely distributed throughout nature and constitute a superfamily of six enzyme families (*1*) (for a comprehensive review, see ref *2*). Recent reviews (*3*, *4*) deal with the catalytic mechanism and active center chemistry of the papain family, which contains the most well-characterized and intensively studied member of the superfamily, papain itself (EC 3.4.22.2), and mechanistically important effects of noncovalent interactions involving this enzyme family continue to be discovered (*5*, *6*).

The nature of the kinetic consequences of electrostatic effects initiated by ionizations various distances from and with different orientations with respect to the catalytic site remains one of the least well understood aspects of enzyme active center chemistry (see, e.g., refs *7* and *8*), and there is considerable evidence that electrostatic effects (*9*) are a major factor in determining the behavior of cysteine proteinases (see, e.g., refs *10*−*16*). The carboxy group of Asp158 in papain is the ionizable group nearest the catalytic site, being

[†] We acknowledge research studentships from the Engineering and Physical Sciences Research Council for S.G., from the Science and Engineering Research Council for M.P.T., and from the Biotechnology and Biological Sciences Research Council for S.H.

* To whom correspondence should be addressed: Laboratory of Structural and Mechanistic Enzymology, School of Biological and Chemical Sciences, Fogg Building, Queen Mary, University of London, Mile End Road, London E1 4NS, U.K. Telephone: 00 (44) 2078826352. Fax: 00 (44) 208 0973. E-mail: kb1@qmul.ac.uk.

[‡] Laboratory of Structural and Mechanistic Enzymology, School of Biological and Chemical Sciences, Fogg Building, Queen Mary, University of London.

[§] Present address: Assay Development, GlaxoSmithKline Research & Development Ltd., New Frontiers Science Park (North), Third Avenue, Harlow, Essex CM19 5AW, U.K.

[||] These authors contributed equally to this paper.

[⊥] Present address: Astra Zeneca, Mereside, Alderley Park, Cheshire SK10 4TG, U.K.

[∞] Present address: Cyclacel Ltd., James Lindsay Place, Dundee DD1 5JJ, U.K.

[@] School of Biological and Chemical Sciences, Walter Bessant Building, Queen Mary, University of London.

[#] Bioinformatics Institute.

[+] University of Salford.

10.1021/bi702126p CCC: $40.75
Published on Web 01/29/2008

separated from the (Cys25)−S^-/(His159)−Im^+H[1] ion pair by approximately 7 Å (*17*), and its role in active center chemistry has long been controversial (*3*, *4*). A major advance in understanding the mechanism of cysteine proteinase-catalyzed hydrolysis resulted from a combination of reactivity probe kinetics, kinetics of catalysis, and electrostatic potential calculations for papain and some natural variants (*18*). The results of these studies showed that (i) the ion pair state produced by protonic dissociation from (Cys25)−SH/(His159)−Im^+H across pK_a 3.35 in papain, 2.90 in caricain [papaya (*Carica papaya*) proteinase Ω, EC 3.4.22.30] (*18*), and 2.70 in actinidin (EC 3.4.22.14) (*4*, *17*), although necessary, is insufficient for catalytic competence, (ii) protonic dissociation from an electrostatic modulator with a pK_a of approximately 4 in papain (and in caricain) (*18*) and a pK_a of 5 in actinidin (*17*) is required for catalysis, (iii) this key modulator cannot be the Asp158 carboxy group in papain and caricain because their pK_a values are known to be 2.8 and 2.0, respectively (*17*, *19*), (iv) in papain and caricain (Asp158)−CO_2^- may be an electrostatic modulator (*12*, *13*) additional to that with a pK_a of 4 (as yet unassigned and probably remote from the immediate active center) but, if so, permanently in the "on" state over the pH range in which catalytic activity develops, and (v) both the electrostatic modulation with a pK_a of approximately 4 and specific hydrophobic P_2-S_2 and $P_1/P_2-S_1/S_2$ intersubsite hydrogen bonding interactions with substrate-derived time-dependent thiol-specific inhibitors contribute to changes in transition state geometry such that the two components of the catalytic site Cys/His ion pair are able to play their catalytic roles of nucleophile and hydrogen bond and proton donor, respectively (see refs *3* and *4* and references cited therein, and ref *11*). In their paper on bleomycin hydrolase, a hexameric member of the papain family, O'Farrel and Joshua-Tor (*6*) emphasize the probable importance of the complex network of structural interactions in the active center regions of members of this enzyme family; at least for bleomycin, such interactions extend far beyond the immediate catalytic site.

This paper illuminates one of the key outstanding problems in understanding the active center chemistry of papain, i.e., the nature of the phenomenon required to generate substantial nucleophilic reactivity in the (Cys25)−S^-/(His159)−Im^+H ion pair by decreasing the level of mutual solvation of the anionic and cationic partners. To investigate this phenomenon, we carried out computer modeling and a pH-dependent kinetic study using a new series of cationic aminoalkyl 2-pyridyl disulfide reactivity probes designed to bind with various degrees of effectiveness near both Asp158 and Trp177 as well as to react with Cys25. The results suggest an important role for movement of Trp177 but not for the electrostatic field of Asp158 in the generation of nucleophilic character in the catalytic site ion pair.

EXPERIMENTAL PROCEDURES

Enzymes and Reactivity Probes. The purification of papain (*20*), including the production of fully active enzyme by covalent chromatography (reviewed in ref *21*), has been

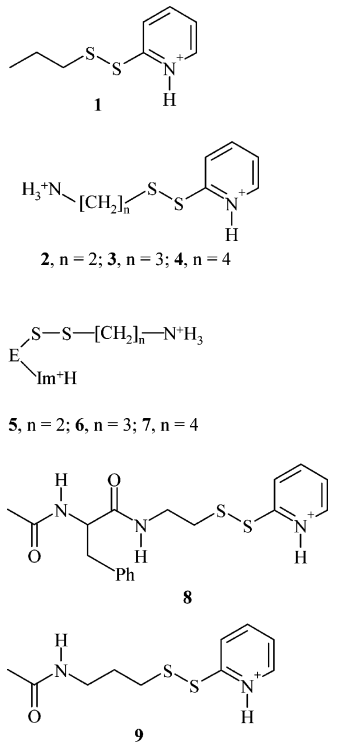

FIGURE 1: The fully protonated cationic forms of the reactivity probes used in the kinetic studies and the derivatized enzyme subjected to computer modeling. *n*-Propyl-2-pyridyl disulfide **1** exists in acidic media as the equilibrium mixture CH_3-$[CH_2]_2$-S-S-2-Py^+H ⇌ CH_3-$[CH_2]_2$-S-S-2-Py; *ω*-aminoalkane 2′-pyridyl disulfides **2**−**4** exist in acidic and weakly alkaline media as the equilibrium mixtures H_3N^+-$[CH_2]_n$-S-S-2-Py^+H ⇌ H_3N^+-$[CH_2]_n$-S-S-2-Py. In **1**−**4**, the protonated pyridyl N atoms have pK_a values of 2.8, and in **2**−**4**, the protonated primary amino groups have pK_a values of 9.6. **5**−**7** were papain (E) derivatized in the computer by reaction of the catalytic site thiolate anion with probes **2**−**4**, respectively, and modeled to assess the probable locations of their alkylammonium cations with respect to Asp158. *N*-Ac-[Phe]-NH-$[CH_2]_2$-S-S-2-Py (**8**) is a close analogue of a specific substrate containing the major recognition sites; *N*-Ac-NH-$[CH_2]_3$-S-S-2-Py (**9**) is probe **3** with the primary amino group acetylated to prevent this amino group from becoming cationic.

described previously, as has determination of its active center content evaluated by spectroscopic titration at 343 nm (ϵ_{343} = 8080 M^{-1} cm^{-1}) using 2,2′-dipyridyl disulfide as a titrant (*22*). The syntheses of *n*-propyl 2-pyridyl disulfide **1** from pyridine-2-thione and *n*-propanesulfenyl chloride (*23*) and 2-(amino)ethyl-2′-pyridyl disulfide (**2**) from pyridine-2-thione and ethane thiolsulfonate (*24*) have been described previously.

*3-(Amino)trimethylene 2′-Pyridyl Disulfide (**3**, Figure 1).* 3-(Amino)trimethylene mercaptan (0.27 g, 3 mmol) in acetic acid (3 mL) was added dropwise with vigorous stirring over 30 min at room temperature to 2,2′-dipyridyl disulfide (1.32 g, 6 mmol) dissolved in acetic acid (10 mL). After the mixture had been stirred for a further 1 h, the acetic acid was removed by repeated rotary evaporation in vacuo, assisted by additions of toluene. The resulting syrup was dissolved in ethyl acetate (5 mL) and subjected to column chromatography [Al_2O_3, Brockman grade I, 150 mesh; elution with an ethyl acetate/methanol mixture (5:1)] to give the required product (150 mg), eluting after pyridine-2-thione and residual 2,2′-dipyridyl disulfide. It was characterized by mass spectrometry, ^1H NMR, and the expected stoichiometry

[1] Abbreviations: Im^+H, imidazolium; Im, imidazole; 2-Py, 2-pyridyl; R, reactivity probe; $[R]_0$, initial concentration of R.

of the release of pyidine-2-thione ($\Delta\epsilon_{343} = 8080\ M^{-1}\ cm^{-1}$) consequent on thiolysis by 2-mercaptoethanol at pH 8.0: MS (EI mode) *m*/*z* 201 [$M^+ + 1$]; $C_8H_{12}N_2S_2$ requires M^+ 200; ^1H NMR (270 MHz, DMSO-d_6 with 20% D_2O) δ 1.92 (tt, $J = 7.40$, 7.02 Hz, 2 H), 2.81 (t, $J = 7.02$ Hz, 2 H), 2.89 (t, $J = 7.4$ Hz, 2 H), 7.21 (ddd, $J = 6.99$, 4.94, 1.65 Hz, 1 H), 7.71−7.81 (m, 2 H), 8.35 (m, 1 H).

*4-(Amino)tetramethylene 2′-Pyridyl Disulfide (**4**, Figure 1).* A solution of the disulfide of 4-(amino)tetramethylene mercaptan (dihydrobromide) synthesized from 1,4-dibromobutane as described in ref *25* (0.74 g, 2 mmol) in water and tris(2-carboxyethyl)phosphine (0.47 g, 2.1 mmol) was brought to pH ∼4.5 by addition of $NaHCO_3$. The reaction mixture was stirred at room temperature for 1 h and then evaporated to dryness in vacuo at <35 °C. The residue was suspended in acetic acid (2.5 mL) and the suspension added dropwise over 30 min to a solution of 2,2′-pyridyl disulfide (1.76 g, 8 mmol) in acetic acid (10 mL). The mixture was stirred for a further 2 h and then evaporated to dryness in vacuo. The residue was suspended in an ice−water mixture (10 mL) and the excess 2,2′-dipyridyl disulfide removed by filtration. The water soluble fraction containing pyridine-2-thione and the desired mixed disulfide **4** was evaporated to dryness. The residue was dissolved in ethyl acetate and subjected to column chromatography as described for compound **3**. Pure **4** (a clear oil) was dried in vacuo over P_2O_5 and characterized as described for **3**: MS (EI mode) *m*/*z* 215 [$M^+ + 1$]; $C_9H_{14}N_2S_2$ requires M^+ 214; ^1H NMR (400 MHz, DMSO-d_6) δ 1.65−1.70 (m, 4 H), 2.78 (t, $J = 7.0$ Hz, 2 H), 2.88 (t, $J = 6.6$ Hz, 2 H), 3.39 (bs, 2 H, NH_2), 7.26 (ddd, $J = 5.84$, 4.80, 1.0 Hz, 1 H), 7.77 (dd, $J = 8.08$, 0.84 Hz, 1 H), 7.85 (ddd, $J = 8.08$, 8.08, 1.84 Hz, 1 H), 8.47 (m, 1 H).

*3-(Acetamido)trimethylene 2′-Pyridyl Disulfide (**9**, Figure 1).* 3-(Amino)trimethylene 2′-pyridyl disulfide (**3**, 150 mg) prepared as described above was acetylated by being dissolved in water (5 mL) containing $NaHCO_3$ (0.5 g), cooled in ice, and supplemented with acetic anhydride (0.20 g, 2 mmol) while being stirred. The required product (**9**) was isolated by extraction with CH_2Cl_2 (2 × 10 mL) and purified by flash chromatography (CH_2Cl_2/ethyl acetate) to provide tlc (ethyl acetate)-homogeneous material which was characterized as described for **3**: MS (EI mode) *m*/*z* 243 (M + 1); $C_{10}H_{14}N_2S_2O$ requires M^+ 242; ^1H NMR (270 MHz, DMSO-d_6) δ 1.90 (tt, $J = 7.30$, 7.00 Hz, 2 H), 2.0 (s, 3 H), 2.85 (t, $J = 7.0$ Hz, 2 H), 3.15 (t, $J = 7.3$ Hz, 2 H), 7.25 (ddd, $J = 7.1$, 4.90, 1.55 Hz, 1 H), 7.70−7.82 (m, 2 H), 8.2 (s, 1 H, NH), 8.5 (m, 1 H).

Stopped-Flow (SF) Kinetics. Kinetic studies on the reactions of the catalytic site thiol group of papain with the reactivity probes (R) were performed by using a Hi-Tech Scientific stopped-flow spectrophotometer, kinetics workstation, and data acquisition and analysis software. Monochromator entrance and exit slits widths were set at 0.5 mm. The sample handling unit was fitted with a UG5 bandpass filter to eliminate stray light and configured for thermostatically controlled temperature cycling. Temperature control was achieved with a Grant LTD6 water bath. Complete absorbance (*A*) versus time (*t*) progress curves for the reactions of the enzymes with the reactivity probes were recorded by monitoring the release of the chromophoric product pyridine-2-thione at 343 nm ($\Delta\epsilon_{343} = 8080\ M^{-1}\ cm^{-1}$). All reactions were carried out under pseudo-first-order conditions for which $[R]_0$ (initial concentration of R) ≫ [enzyme] at 25 °C in aqueous buffer at $I = 0.1$ M and containing 1 mM EDTA. Pseudo-first-order rate constants (k_{obs}) were computed by fitting the $A-t$ data to an equation for a single-exponential process, i.e., $A = P_1e^{-P_2t} + P_3$, where $P_1 = A_\infty - A_o$, $P_2 = k_{obs}$, and $P_3 = A_\infty$. In all cases, an average of at least three essentially superimposable traces was used to provide k_{obs} (SD < 10%). The linear dependence of k_{obs} (s^{-1}) on $[R]_0$ demonstrated overall second-order kinetics at lower values of $[R]_0$, and the second-order rate constants (k) were obtained by dividing k_{obs} by $[R]_0$. Use of higher values of $[R]_0$ provided evidence for the formation of enzyme−probe adsorptive complexes (ER) prior to covalency change in some cases as hyperbolic saturation curves of k_{obs} versus $[R]_0$. Values of the characterizing parameters, K_r and k_{+2} of the equation $k_{obs} = k_{+2}[E]_T[R]_0/(K_r + [R]_0)$, were obtained by weighted nonlinear regression of k_{obs} on $[R]_0$ assuming constant relative error with weights inversely proportional to k_{obs}^2.

Computer evaluation of pH-dependent kinetic data was carried out by a combination of curve sketching using the multitasking application program SKETCHER and weighted nonlinear regression using Sigmaplot 5.0 (Jandel Scientific) as described in ref *18* and references cited therein. SKETCHER permits rapid evaluation of characterizing parameters in the generic set of equations for various kinetic models differing in the number and reactivity of the reactive states by interactive manipulation of calculated curves.

*Computer Modeling of Papain Derivatized by Reactions with the Cationic Probes **2**−**4** (Figure 1) and of the Transition States of the Reactions with Probes **1**−**4**.* The crystal structure of papain (*26*), initially that in the Brookhaven Protein Data Bank (entry 9pap) with the blocking group bonded to S^γ of the catalytic site Cys25 removed, was used as the basis for modeling. Gln residues 47, 118, and 135 were redefined as Glu (*27*). Buried crystallographic water molecules (*26*) were retained. All residues were assumed to be in their fully charged states (i.e., Arg, Lys, and N-termini with charges of +1 and Asp, Glu, and C-termini with charges of −1). The catalytic site side chains of Cys and His had charges of −1 and +1, respectively, as required for the ion pair state. The CHARMM force field (*28*) was used to establish the modeled structure as described in ref *8*. Hydrogen atoms were built and their orientations optimized along with the orientations of Asn, Gln, and His side chains to maximize hydrogen bonding potentials using the HBUILD (*28*) module of CHARMM. Probes **2**−**4** were constructed by using the EDITOR module of QUANTA and docked in the active center of papain initially as the mixed disulfide products of their reactions with the catalytic site sulfur atom. The amino group of each covalently bonded probe fragment was protonated. Optimal orientations of the docked ligands were achieved by performing conformational searches involving the rotation of the ligand−Cys25 moiety around defined torsional angles followed by extensive energy minimizations until the change in the potential energy gradient was 0.01 kcal mol^{-1} $Å^{-1}$. The lowest-energy conformations of Cys25 and the covalently bonded ligands were then subjected to molecular dynamics simulations. The resulting lowest-energy conformations were solvated, and the systems were again energy minimized until the change in

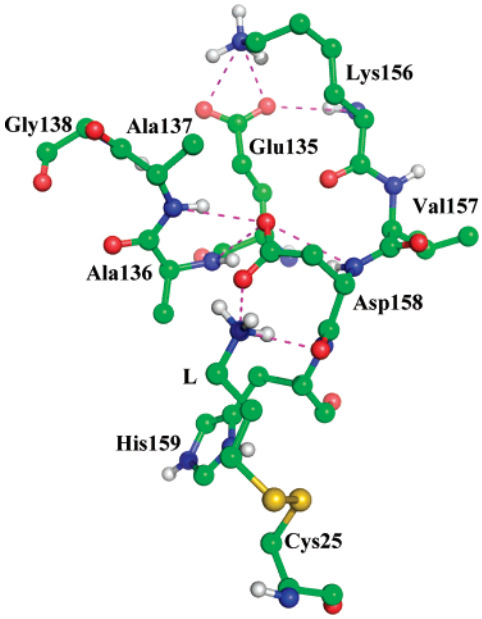

FIGURE 2: Modeled structure of the catalytic site region of papain chemically modified **6** by reaction of the catalytic site thiolate side chain of Cys25 with 3-(amino)trimethylene 2′-pyridyl disulfide **3**. The relevant hydrogen bonding interactions are described in the text: C, green; N, blue; S, yellow; O, red; and H and ligand (L), white. This figure and Figure 7 were produced by using PyMol (*37*).

the potential energy gradient was 0.01 kcal mol^{-1} Å^{-1}. Analogous modeling was carried out to examine a structure approximating the transition state of the thiol−disulfide interchange reaction (quasi-transition state). For this, the complete dicationic forms of probes **2**−**4** were used with the S atom of Cys25 bonded to the S atom of the probe distal from the protonated pyridyl ring.

Normal Mode Analysis. Normal mode calculations (see ref *29*) were used to investigate the ways in which the different orientations of the dicationic forms of probes **2**−**4** in the quasi-transition states of their reactions with papain affect the movement of Trp177. The minimum energy structures were minimized until the energy gradient was less than 10^{-5} kcal mol^{-1} Å^{-1}. This was followed for each system by diagonalizing the matrix of the second derivative of the energy which results in a set of eigenvalues and eigenvectors. The eigenfrequencies translate into the amplitudes of collective motions of the ensemble of atoms, while the eigenvectors indicate the directions of these motions. The full spectrum of 3*N* vibrational modes (where *N* is the number of atoms) was computed for each quasi-transition state. Each normal mode was then projected onto a virtual vector created to represent the region of the protein across Trp177. For this process, we chose two atoms, C^{α}s of Asn18 and Gln148, one on either side of Trp177, and the dotproducts of the two vectors were calculated to assess the perturbation of the region across Trp177. The larger the value of the dotproduct, the more aligned are the two vectors, and the motion along that particular normal mode is identified as the motion that perturbs the region across Trp177.

RESULTS

Variation in Papain−Probe Binding Interactions Involving Asp158 Identified by Modeling the Products of Chemical Reaction. The first part of the modeling program involved assessment of whether the distance between the ω−N^+H_3 substituent of the probe and its electrophilic center was consistent with some or all of the cationic reactivity probes **2**−**4** (Figure 1) potentially engaging Asp158 in addition to undergoing chemical reaction with Cys25. To this end, we modeled the structures of the products of the thiol−disulfide interchange reactions, **5**−**7** (Figure 1), and the results, described below, are exemplified in Figure 2 by the product **6** of the reaction with probe **3**. The proximity of the side chain of Cys25 to the electrophilic centers of the probes was ensured by modeling the product of the thiol−disulfide interchange reaction after departure of the mercaptopyridine leaving group.

Table 1: Kinetic Parameters for the Reactions of Papain with Three Aminoalkyl 2-Pyridyl Disulfides (**2**−**4**) at 25 °C, pH 6.6, and I = 0.1 M[a]

disulfide	k_{+2} (s^{-1})	K_r ($\times$**10**^{3} M)	k_{+2}/K_r ($\times$**10**$^{-3}$ M^{-1} s^{-1})
H_3N^+-$[CH_2]_2$-S-S-2-Py **2**	9.0 ± 1.0	1.73 ± 0.23	5.20
H_3N^+-$[CH_2]_3$-S-S-2-Py **3**	3.2 ± 0.1	0.36 ± 0.02	8.89
H_3N^+-$[CH_2]_4$-S-S-2-Py **4**	2.0 ± 0.1	0.67 ± 0.06	2.99

[a] The parameters relate to the model in eq 1 of the text where k_{+2} is the rate constant for the formation of the chemically modified enzyme E_{mod} and K_r, the value of the disulfide concentration when $k = k_{+2}/2$, is the steady state assembly $(k_{-1} + k_{+2})/k_{+1}$. This closely approximates k_{-1}/k_{+2} in view of the low values of k_{+2}/K_r relative to the probable lower limit of the value of k_{+1}; the conventional condition for quasi-equilibrium ($k_{+2} \ll k_{-1}$) is a necessary consequence of the condition k, i.e., $k_{+2}/K_r \ll k_{+1}$ (*31*). At pH 6.6, the disulfides exist predominately with the primary amino group protonated and the pyridyl N atom unprotonated.

In papain chemically modified by reaction with probe **2**, the $-N^+H_3$ group of the ligand [which is separated from the sulfur atom of Cys25 (**5**) by two methylene groups] is engaged in hydrogen bonding interaction with the backbone carbonyl oxygen of Asp158. The closest approach of the $-N^+H_3$ group to the carbonyl oxygen of Asp158 is 2.7 Å. The orientation of Asp158 is not substantially perturbed as its side chain continues to make a hydrogen bond with the backbone N−H group of Ala137 and does not interact with the $-N^+H_3$ group of the ligand. In papain chemically modified by reaction with probe **3**, in which the $-N^+H_3$ group is further separated from the sulfur atom of Cys25 by an additional methylene group (**6**), the $-N^+H_3$ group engages in interaction not only with the backbone carbonyl oxygen of Asp158 but also with its carboxylate side chain (Figure 2). The closest approach of the $-N^+H_3$ group to the carbonyl oxygen is 2.7 Å, and that to one of the carboxylate oxygens is 2.5 Å. As with **5**, the orientation of Asp158 is not substantially perturbed as its side chain continues to accept a hydrogen bond from the backbone N−H group of Ala137. The additional interactions between papain and the $-N^+H_3$ group of the probe in **6** which do not occur in **5** suggest that binding of the longer probe **3** containing the three-methylene spacer might be more effective than the binding of the shorter probe **2** with the two-methylene spacer. When the enzyme is derivatized with the even longer probe **4** with the four-methylene spacer as in **7**, the hydrogen bonding with the backbone carbonyl and the electrostatic interaction with the carboxylate side chain of Asp158 are maintained. The side chain of Asp158 is reoriented to accommodate the longer

ligand, and this results in the formation of an additional hydrogen bond between (Asp158)−CO_2^- and the backbone N−H group of Ala136.

*Kinetic Evaluation of the Binding to Papain of the Monocationic Forms of Reactivity Probes **2**−**4***. By contrast with reactions of papain with probes containing noncationic side chains such as **1**, **8**, and **9** (see the Discussion), it was possible to demonstrate substantial degrees of saturation by the monocationic forms of **2**−**4**. The characterizing parameters of these kinetic saturation curves are listed in Table 1. By carrying out these reactions at pH 6.6, we were able to ensure that the only positive charge on each of the probe molecules resided on the primary amino group because the pK_a value of the substituted pyridinium cation is 2.8 and that of the substituted primary ammonium cation is 9.6. A typical kinetic saturation curve, that for the reaction of papain with 3-(amino)trimethylene 2′-pyridyl disulfide (**3**), is shown in Figure 3A. Figure 3B demonstrates the lack of observable saturation in the reaction of papain with 3-(acetamido)trimethylene 2′-pyridyl disulfide **9** in which the relevant positive charge in **3** has been removed by acetylation.

pH-Dependent Kinetic Studies. The pH-dependent kinetic studies of the reactions of the catalytic site thiol group of papain (Cys25) with *n*-propyl 2-pyridyl disulfide **1** and with the aminoalkyl 2-pyridyl disulfide probes **2**−**4** were undertaken to assess the effects on its reactivity characteristics of binding interactions of both the ω-N^+H_3 groups and the pyridyl rings. The expectation was that the latter might occupy space near Trp177, at least in some cases. Nucleophilic character in the (Cys25)−S^-/(His159)−Im^+H ion pair is readily recognized in the presence of a striking rate maximum at pH ∼4 associated with reaction of the probe with its pyridyl ring protonated. The reactions were carried out under (pseudo) first-order conditions where $[R]_0 \gg [E]_T$ but over a range of $[R]_0$ values such that the increase in k_{obs} with the increase in $[R]_0$ closely approximated linearity; i.e., $[R]_0 \ll K_r$. This provided for the dependence of k_{obs} on free reactant state pK_a values, i.e., those of the free enzyme and free probe molecules (*30*). In terms of the adsorptive complex model, eq 1, the significance of the pH-dependent second-order rate constant (k) obtained as $k_{obs}/[R]_0$ is k_{+2}/K_r, where $K_r = k_{-1}/k_{+1}$ (*31*). Studies using probes **2**−**4** were restricted to the pH range of approximately <8 to avoid complications from alkaline hydrolysis.

$$E + R \underset{k_{-1}}{\overset{k_{+1}}{\rightleftharpoons}} ER \xrightarrow{k_{+2}} E_{mod} + P \qquad (1)$$

As a benchmark probe molecule to assess the influence of the ω-N^+H_3 group, *n*-propyl 2-pyridyl disulfide **1**, in which CH_3 replaces the 2-amino group in **2**, was included in the study. The pH−k profile for the reaction of papain with **1** is shown in Figure 4A. The solid line corresponds to eq 2 (see ref *32*) which relates to Figure 5. As expected from previous results obtained with 2,2′-dipyridyl disulfide and simple alkyl 2-pyridyl disulfides (see refs *3* and *4*), the main features of the profile are a striking bell-shaped component in acidic media, a rate minimum in approximately neutral media, and a small increase in k toward a reactivity plateau at high pH. The broken lines in Figure 4 correspond to contributions to

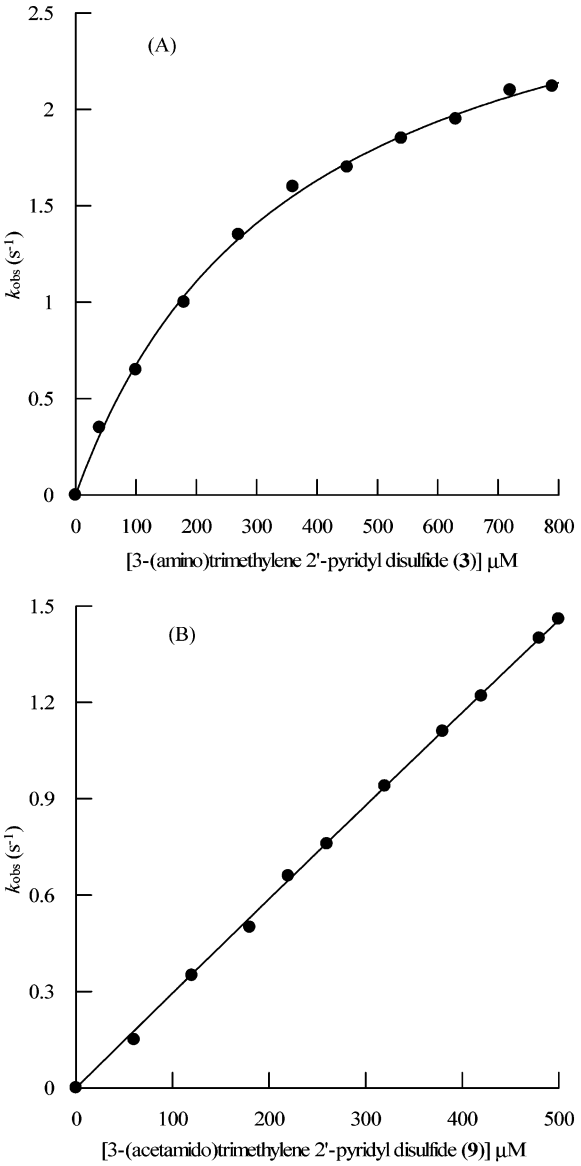

FIGURE 3: Demonstration of (A) saturation kinetics for the reaction of papain with 3-(amino)trimethylene 2'-pyridyl disulfide **3** at 25 °C, pH 6.6, and I = 0.1 M and (B) the lack of observable saturation in the analogous reaction with 3-(acetamido)trimethylene 2′-pyridyl disulfide **9**. In both panels A and B, the data points are mean values of at least three determinations with standard deviation values of <±10% of the means (see Experimental Procedures), and the solid lines are (A) theoretical for model 1 and $k_{+2} = 3.2 \pm 0.1$ s^{-1} and K_r ($=k_{-1}/k_{+1}$) = (3.6 ± 0.2) × 10^{-4} M and (B) a bimolecular reaction obeying second-order kinetics with k = (3.0 ± 0.1) × 10^3 M^{-1} s^{-1}.

k from individual protonic states (Figure 5) (the four terms of the right-hand side of eq 2) which are discussed below for Figure 4A in relation to the molecular components of Figure 6. Three of the macroscopic pK_a values required to fit the solid line in Figure 4A to the data (2.7, 3.35, and 4.1) result from the mixing of the known pK_a values of the pyridinium ring of the probe (2.8), the first pK_a of the (Cys25)−SH/(His159)−Im^+H pair (3.35) and the pK_a of the unknown modulator required in its dissociated state for catalytic activity (4.0). The pK_a for formation of the Cys/His ion pair (3.35) is only approximately 0.6 higher than that for deprotonation of the probe. The observed macroscopic pK_I, therefore, is lowered to 2.7. The value of pK_{II}

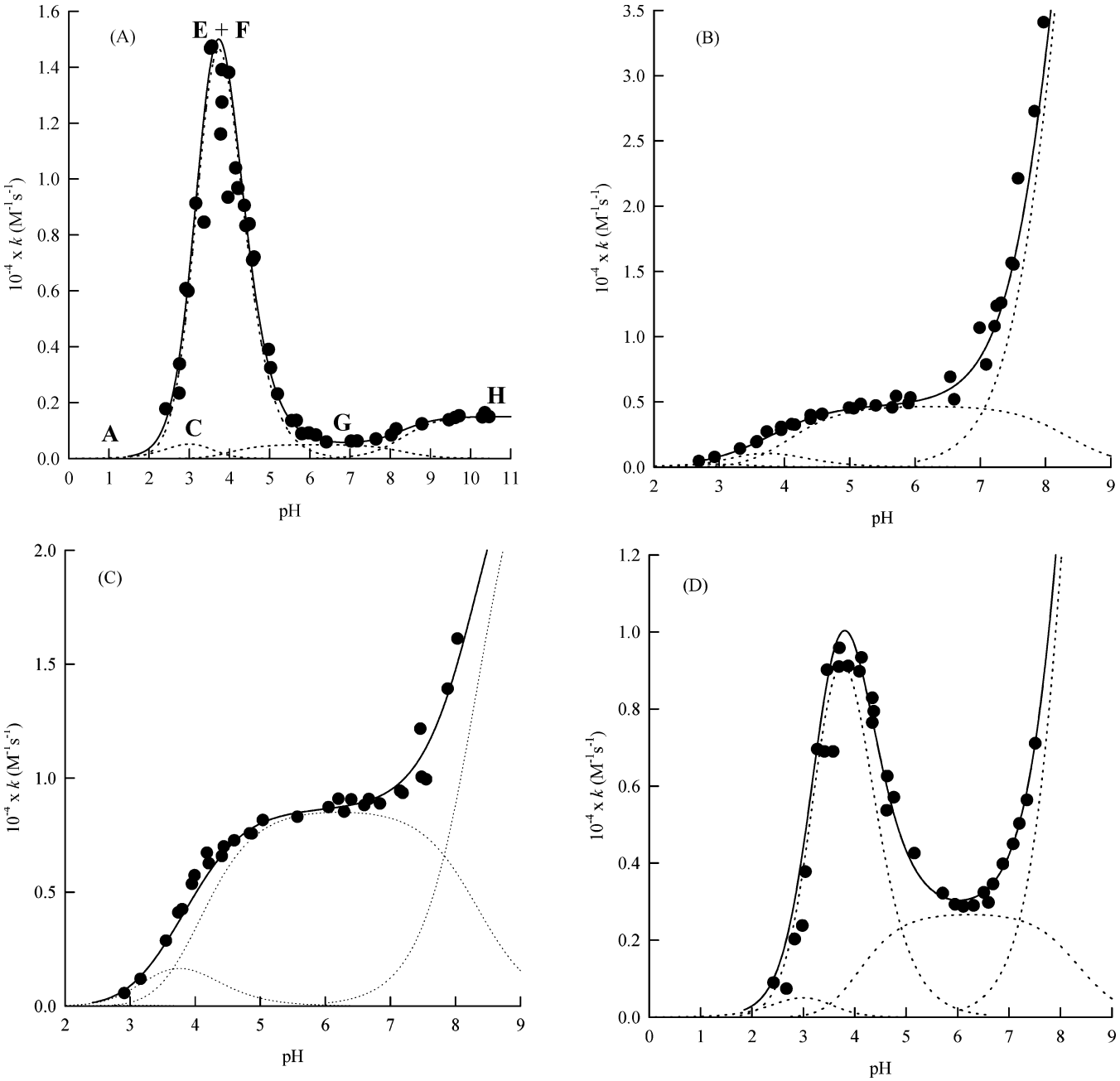

FIGURE 4: pH dependences of the second-order rate constants (k) for the reactions at 25 °C and $I = 0.1$ M of papain with (A) *n*-propyl 2-pyridyl disulfide **1**, (B) 2-(amino)ethyl 2′-pyridyl disulfide **2**, (C) 3-(amino)trimethylene 2′-pyridyl disulfide **3**, and (D) 4-(amino)-tetramethylene 2′-pyridyl disulfide **4**. In all cases. the pH and k data points are mean values of at least three determinations of k at a given pH with standard deviation values of $<\pm 10\%$ of the means (see Experimental Procedures), and the solid lines are theoretical for eq 2 (Figure 5). The values of the characterizing parameters, macroscopic pK_a values (pK_I−pK_{IV}) and pH-independent rate constants ($\tilde{k}_1$−$\tilde{k}_4$ in M^{-1} s^{-1}), are given below. The broken lines correspond to contributions to k of the individual protonic states of the reactions provided by the individual terms of the right-hand side of eq 2, the molecular components of which are shown in Figure 6. In all cases, the solid line is shown with p$K_I = 2.7$, p$K_{II} = 3.35$, p$K_{III} = 4.1$, and p$K_{IV} = 8.3$. (A) $\tilde{k}_1 = 1.0 \times 10^3$, $\tilde{k}_2 = 2.7 \times 10^4$, $\tilde{k}_3 = 5.0 \times 10^2$, $\tilde{k}_4 = 1.5 \times 10^3$. (B) $\tilde{k}_1 = 4.0 \times 10^2$, $\tilde{k}_2 = 2.0 \times 10^3$, $\tilde{k}_3 = 4.7 \times 10^3$, $\tilde{k}_4 = 9.0 \times 10^4$. (C) $\tilde{k}_1 = 63$, $\tilde{k}_2 = 3.1 \times 10^3$, $\tilde{k}_3 = 8.6 \times 10^3$, $\tilde{k}_4 = 2.8 \times 10^4$. (D) $\tilde{k}_1 = 10$, $\tilde{k}_2 = 1.7 \times 10^4$, $\tilde{k}_3 = 2.7 \times 10^3$, $\tilde{k}_4 = 3.7 \times 10^4$. In panel A, **C**, **E** + **F**, **G**, and **H** relate to the reactive components formed from the unreactive component, **A**, as shown in Figure 6.

(3.35) remains essentially similar to that for ion pair formation because it is increased by 0.1 by mixing with a pK_a of 2.8 and lowered by about the same amount by mixing with a pK_a of 4.0 which is itself increased to 4.1. The pK_a value (4.0) of the unknown essential modulator (*18*) (XH in Figure 6) suggests that it might be a carboxy group but cannot be (Asp158)−CO_2H because the pK_a of this side chain is known to be 2.8 (*19*).

The pH−k profile for the reaction of papain with H_3N^+-$[CH_2]_2$-S-S-2-Py (**2**), in the pH range of ∼3−8, where the $-N^+H_3$ group (p$K_a = 9.6$) is maintained, is shown in Figure 4B. A particularly marked difference between this pH−k profile and that for **1** in Figure 4A is the lack of the striking bell-shaped component centered on pH ∼4 in the former. The lack of this bell compels the view that reaction with the activated form of probe **2** protonated on the pyridyl ring and

$$k = \tilde{k}_1/[1 + [H^+]/K_I + K_{II}/[H^+] + (K_{II}K_{III})/[H^+]^2 + (K_{II}K_{III}K_{IV})/[H^+]^3] + \tilde{k}_2/[1 + [H^+]^2/(K_IK_{II}) + [H^+]/K_{II} + K_{III}/[H^+] + (K_{III}K_{IV})/[H^+]^2] + \tilde{k}_3/[1 + [H^+]^3/(K_IK_{II}K_{III}) + [H^+]^2/(K_{II}K_{III}) + [H^+]/K_{III} + K_{IV}/[H^+]] + \tilde{k}_4/[1 + [H^+]^4/(K_IK_{II}K_{III}K_{IV}) + [H^+]^3/(K_{II}K_{III}K_{IV}) + [H^+]^2/(K_{II}K_{IV}) + [H^+]/K_{IV}] \quad (2)$$

necessarily, therefore, doubly protonated, i.e., H_3N^+-$[CH_2]_2$-S-S-2-Py^+H, does not occur. Thus, reactions analogous to those in components C and F of Figure 6 for **1** do not occur with **2**. The same conclusion applies to the reaction of papain with **3**, for which the pH−*k* profile (Figure 4C) also lacks the bell-shaped component centered at pH ∼4. In marked contrast to panels B and C of Figure 4, the bell-shaped component centered on pH ∼4 is restored in Figure 4D when the cationic ammonium group is further separated from the reaction center as in probe **4**.

*Variation in Enzyme−Probe Binding Modes in the Quasi-Transition States of the Reactions of Papain with Probes **1**−**4** at Low pH.* This part of the modeling program was carried out with the dicationic forms of **2**−**4** and the cationic form of **1**. The binding modes deduced, therefore, are those relevant to reaction of the ion pair of papain with each probe containing the 2-mercaptopyridine leaving group activated by protonation. This enables it to act as a sensitive detector of nucleophilic character in the Cys25 component of the catalytic site ion pair as described above.

The striking result is that in the quasi-transition states for the reactions of the amino-containing probes with $n = 2$ (**2**) and $n = 3$ (**3**) the pyridyl ring is bound near the indole ring system of Trp177 (panels A and B of Figure 7, respectively), whereas in those for the reactions of the analogous probe with $n = 4$ (**4**) and the non-amino-containing probe (**1**), the pyridyl ring is bound remotely from Trp177 (panels C and D of Figure 7, respectively). In the case of **2**, its $-N^+H_3$ group makes a hydrogen bond with the backbone carbonyl O atom of Asp158 and its protonated pyridyl ring is bound close to the six-membered component of the indole ring system such that the N^+H group makes a hydrogen bond with the side chain of Asp158. The $-N^+H_3$ group of **3** is also hydrogen bonded to the backbone carbonyl O atom of Asp158, but the necessity to accommodate the additional

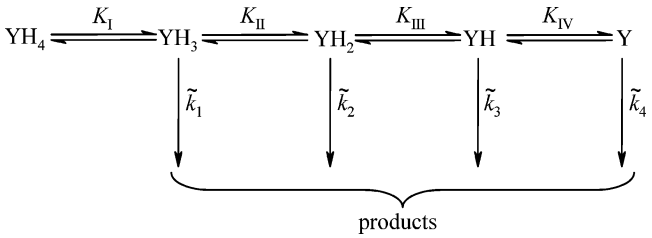

FIGURE 5: Kinetic model and the associated pH-dependent rate equation for reactions in four protonic states. In the model, YH_4-Y represent generalized reactant protonic states with charges omitted; YH_3-Y are reactive, and YH_4 is unreactive. K_I-K_{IV} are macroscopic acid dissociation constants, and $\tilde{k}_1-\tilde{k}_4$ are pH-independent rate constants. Rate equations for reactions in any number of protonic (hydronic) states may be written down without the need for extensive algebraic manipulation by using a simple general expression and two information matrices (see ref *32*). Equation 2 (see the Results) is for reaction in four protonic states.

methylene group of the probe results in the protonated pyridyl ring being close to the five-membered ring of Trp177 and the movement of (Cys25)−S^- away from (His159)−Im^+H by 0.8 Å. In the case of **4**, its methylene chain is too long to "bunch up" and allow the $-N^+H_3$ group to hydrogen bond to Asp158. Instead, it finds a minimum with the protonated pyridyl ring pointing away from Trp177 into the groove of the binding site that accommodates specific peptide substrates. The $-N^+H_3$ group hydrogen bonds with the backbone carbonyl O atom of Cys22, and this causes the S of the probe bonded to (Cys25)−S to be ∼0.8 Å farther from Trp177 than is the case with probe **3**. The position of the (Cys25)−S is essentially unperturbed, and its distance from (His159)−Im^+H is similar to that in papain itself. The N^+H group of the pyridyl ring is ∼4.3 Å from the nearest hydrogen bond acceptor, the backbone carbonyl O atom of Gly23, but is in a dynamic ensemble and will probably hydrogen bond with it. The binding mode of **1** is similar to that of **4**. The protonated pyridyl rings of **2** and **3** are bound in the proximity of the indole ring system of Trp177. By contrast, this is not the case for either **1** or **4**. The significance of this difference is its correlation with the observation that nucleophilic character in the Cys25/His159 ion pair in acidic media is detected by probes **1** and **4** (panels A and D of Figure 4, respectively) but not by **2** and **3** (panels B and C of Figure 4, respectively).

Normal Mode Analysis of Motions in the Vicinity of Trp177. The system containing probe **4** is characterized by an overall normal mode frequency spectrum that is red-shifted relative to that containing probe **2**, indicating lower-frequency and thus larger-scale motions for the latter. This suggests that the global modes of motion in the former are softer, i.e., more easily deformable and larger in amplitude than those in the latter. Mode 10 (frequency of 5.3 cm^{-1} for both systems) was found to have the highest dotproduct value, and this was 5-fold larger for that containing **4** than for that containing **2**. In the motion for the latter, the movement of Trp177 is contained within the moving walls of the active center cleft around it. It swivels and presses onto His159, thereby retaining the mutual solvation with Cys25. By contrast, in the former, the motion of the cleft around Trp177 is antisymmetric with an open−close motion around the Trp177 region. Trp177 glides over His159 and results in the imidazolium side chain being exposed to solvent.

DISCUSSION

A key event in the catalytic mechanism of papain is necessarily the perturbation of the geometry of the intimate (Cys25)−S^-/(His159)−Im^+H ion pair to release the nucleophilic character of the thiolate anion known to occur in acidic media at a pH lower than where catalytic activity develops (*18*). Evidence has been reported previously that this initial event is followed by further perturbation of the Cys25/His159 ion pair that results in the reorientation of the thiolate anion and imidazolium cation components required for nucleophilic attack at the carbonyl C atom of the substrate and the association of the imidazolium cation with the leaving group. The reorientation appears to result from the combined effects of the yet unassigned ionization with a pK_a of 4, across which k_{cat}/K_m increases (*18*), and specific P_2/S_2 and transcleft binding (*3*, *4*, *11*). By contrast, the origin of the initial

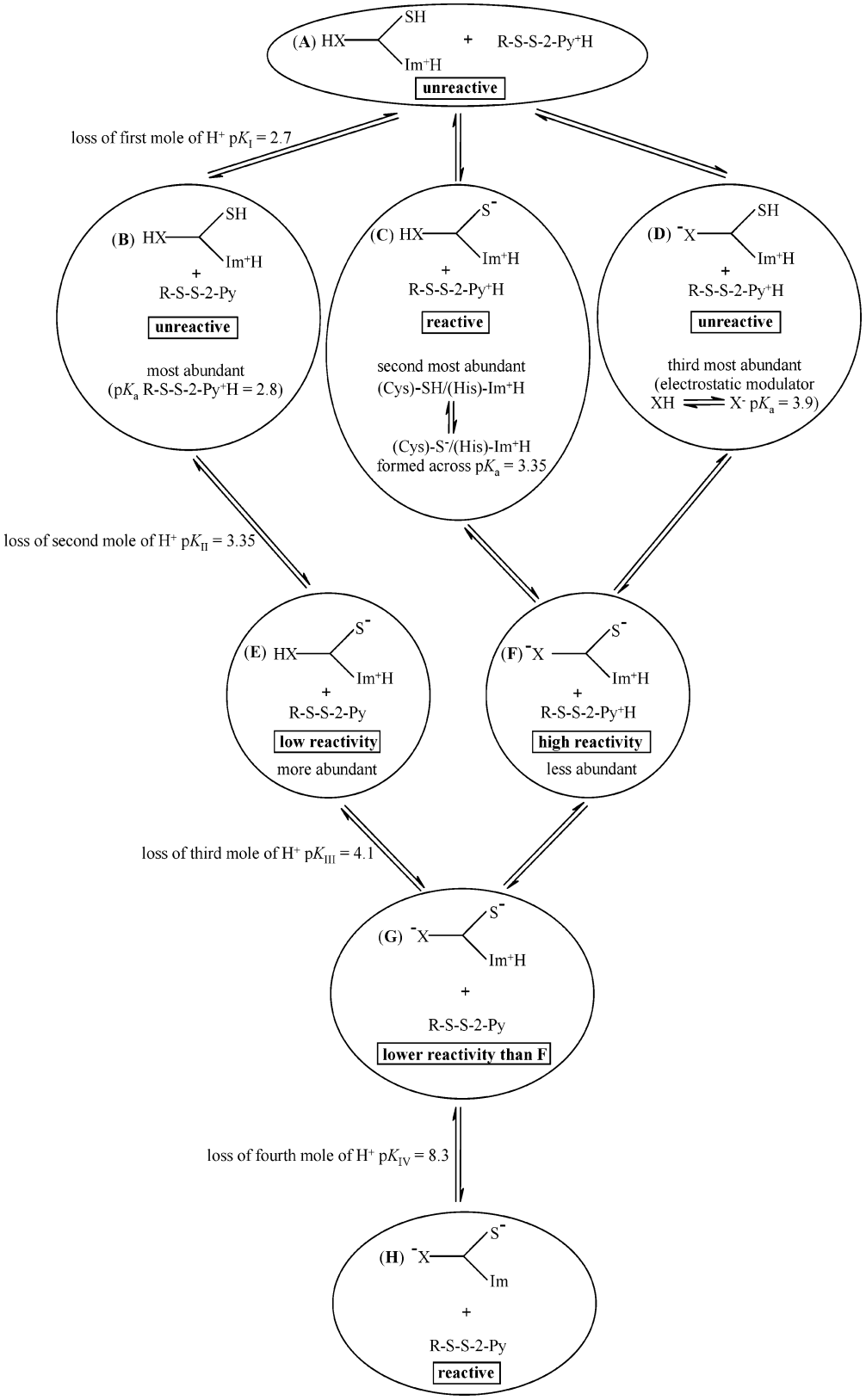

FIGURE 6: Generation of the reactive components in the reaction of Cys25 of papain with *n*-propyl 2-pyridyl disulfide **1** in its protonated and deprotonated forms (R-S-S-2-Py$^+$H ⇌ R-S-S-2-Py). R = $CH_3[CH_2]_2$. SH, Im$^+$H, and XH are kinetically significant groups contributed by Cys25, His159, and the unknown electrostatic modulator (*18*) of papain, respectively. Reactivity is considered to require $-S^-$. R-S-S-2-Py$^+$H is approximately 1000 times more reactive then R-S-S-2-Py. Deprotonation of the unknown XH group (possibly a carboxy group other than Asp158) increases both the reactivity of the ion pair and k_{cat}/K_m. The pK_a for ion pair formation (3.35) is only ~0.6 greater than that for the deprotonation of CH_3-$[CH_2]_2$-S-S-2-Py$^+$H (pK_a = 2.8); the value of the observed macroscopic pK_I, therefore, is depressed to 2.7. The value of pK_{II} (3.35) remains essentially the same as that for ion pair formation because it is increased by 0.1 as a result of mixing with a pK_a of 2.8 and decreased by approximately the same amount by mixing with the pK_a of 4.0 which itself is increased to 4.1; for further details, including the use of modifications of this figure to describe pH−k profiles of the reactions of papain with H_3N^+-$[CH_2]_n$-S-S-2-Py (n = 2−4 for amino probes **2**−**4**, respectively), see the text.

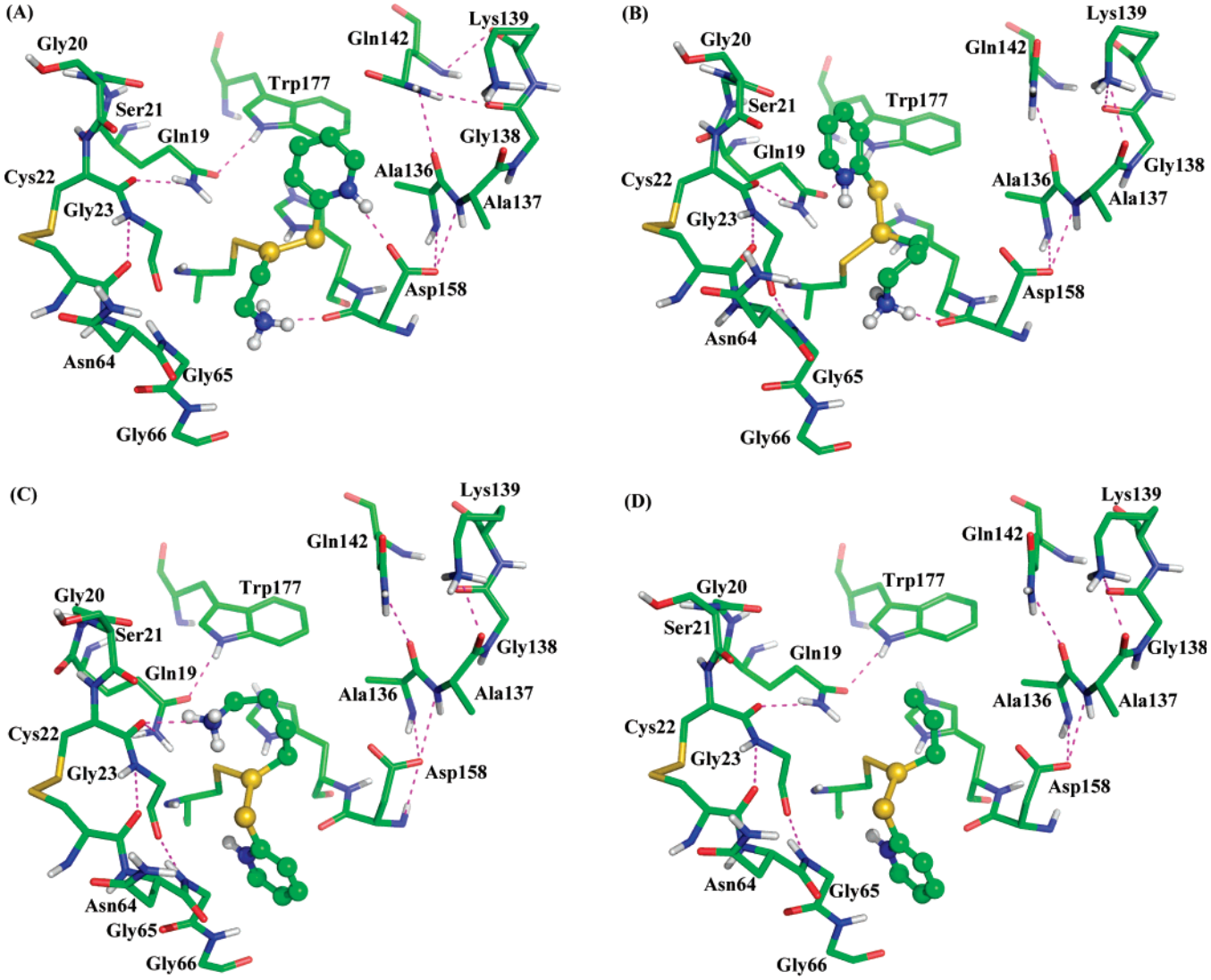

FIGURE 7: Modeled structures of the quasi-transition states of the reactions of papain with (A) amino probe **2**, (B) amino probe **3**, (C) amino probe **4**, and (D) propyl probe **1**. The atoms of the probes are shown as spheres: C, green; N, blue; S, yellow; and H, white. Selected amino acid residues of papain are labeled with the three-letter code. The binding modes of the four probes are discussed in the text.

generation of nucleophilic character was yet to be established. In this work, potential contributions by Asp158 and Trp177 were investigated.

The possibility of a contribution by the carboxylate anion of Asp158 was investigated initially by modeling enzyme−reactivity probe combinations and kinetic analysis. Modeling of the covalent products **5** (Figure 1) of reaction of Cys25 with the aminoalkyl 2-pyridyl disulfide probes **2**−**4** demonstrated the possibility of simultaneous binding of the protonated primary amino group to Asp158 and nucleophilic attack of (Cys25)$-S^-$ at the electrophilic S atom of the probe distal from the pyridyl ring. The nature of the interaction with the Asp158 residue varies with the length of the polymethylene spacer. In the case of the product of the reaction with probe **3**, the $-N^+H_3$ group interacts with both the carboxylate side chain of Asp158 and its backbone carbonyl O atom (Figure 2), and this is true also for the product of the reaction with probe **4**. By contrast, the $-N^+H_3$ group of the product of the reaction with probe **2** interacts with the backbone carbonyl O atom of Asp158 but not with its carboxylate side chain. Binding predicted by the modeling was demonstrated by the saturation kinetics observed in the k_{obs} versus [probe] plots for the reactions of all three of the monoprotonated probes **2**−**4** at pH 6.6. These results contrast with the lack of observable saturation (i.e., where the k_{obs} vs [probe] relation is linear) in the reaction of 3-(acetamido)-trimethylene 2′-pyridyl disulfide **9** in which the relevant positive charge in **3** has been removed by acetylation. A lack of observable saturation was found also for the reaction of the *n*-propyl probe **1** in which the $-N^+H_3$ group is replaced with CH_3.

The reactions of a number of noncationic 2-pyridyl disulfide probes (R) with cysteine proteinases, with R in substantial excess over E, have been shown previously to obey (pseudo) first-order kinetics (k_{obs}) with respect to time and second-order kinetics with respect to concentration up to the solubility limit of the probe which is the case with **9** (Figure 3B) (see, e.g., ref *33* and references therein). Although kinetic study of these reactions, therefore, provided no evidence for an adsorptive complex ER prior to covalency change, in terms of eq 1 the second-order rate constant, k, can be regarded as k_{+2}/K_r, where $K_r = k_{-1}/k_{+1}$ when quasi-equilibrium around ER applies (*31*). Even when the major recognition features were incorporated into the probe mol-

ecule, i.e., **8**, evidence for ER could not be obtained kinetically because the reactions are sufficiently fast that equimolar concentrations of E and R are required to monitor progress curves on the stopped-flow time scale. By contrast, in this work, it was possible to demonstrate substantial degrees of saturation of papain by the monocationic forms of probes **2**−**4**, each containing the protonated ω-amino group and the unprotonated pyridyl ring. As might be expected, the demonstrable binding of the cationic probes results in the values of k_{+2}/K_r (in M^{-1} s^{-1}) for their reactions at pH 6.6 (5.2×10^3, 8.9×10^3, and 3.0×10^3) that are all substantially greater than the value of the equivalent parameter k (the second-order rate constant) for the reaction of the noncationic probe *n*-propyl 2-pyridyl disulfide (**1**) (5.0×10^2 M^{-1} s^{-1}; see Figure 4A). The value of K_r for probe **3** which interacts electrostatically with the Asp158 carboxylate is approximately 5 times smaller than the K_r for probe **2** which binds only to the backbone carbonyl oxygen. Although (k_{+2} for **2**)/(k_{+2} for **3**) = 2.8, the overall effectiveness of the reaction of papain with **3** (which eliminates any effect of nonproductive binding modes) is somewhat greater than that for reaction with **2** [(k_{+2}/K_r for **3**)/(k_{+2}/K_r for **2**) = 1.7].

The existence of demonstrable binding of probes **2**−**4** and differences in the binding modes around Asp158 in the reaction products suggested that more extensive study might illuminate the origin of the nucleophilic character in the Cys25/His159 ion pair. This proved to be the case when detailed pH-dependent kinetics and modeling of the transition states of the reactions of the dicationic forms of the amino-containing probes were carried out. Modeling of the transition states provided the key to understanding the origin of nucleophilic character in the catalytic site ion pair. This was not apparent from modeling the enzyme−probe disulfide products because of the variation in binding modes subsequently shown to be dictated by interactions involving the protonated pyridyl ring of the leaving group and their role in inhibition of the development of nucleophilicity.

The striking differences between the pH−*k* profiles for the reactions of papain with probe **1** and the longest amino-containing probe **4** (panels A and D of Figure 4, respectively) and those for the reactions of the probes of intermediate length (**2** and **3** in panels B and C of Figure 4, respectively) proved to be decisive in identifying the enzyme−probe interactions that determine the presence or absence of nucleophilic character in Cys25 at low pH. The existence of nucleophilic character in Cys25 is readily demonstrated using simple alkyl 2-pyridyl disulfide probes by the presence of a bell-shaped component with high reactivity at low pH in the pH−*k* profiles (*33*). In this work, this was reinforced by new data for the reaction of probe **1** (Figure 4A), explained in Figure 6. Protonation of the pyridyl ring provides the probe with enhanced reactivity which makes it a sensitive detector of nucleophilic character. The lack of the high-reactivity bells in the pH−*k* profiles for the reactions of probes **2** and **3** (panels B and C of Figure 4, respectively) demonstrates the absence of nucleophilic character in Cys25 toward these probes protonated on the pyridyl ring. The absence of these low-pH bells and the presence of this feature in Figure 4D for the reaction of the longest of the amino-containing probes (**4**) provided the opportunity by modeling to identify the binding modes of the dicationic forms of **2** and **3** associated with loss of nucleophilic character in Cys25 at low pH.

Modeling of the quasi-transition states of the reactions of papain with the four reactivity probes **1**−**4** as described in Experimental Procedures produced a clear basis detailed in the Results for the interpretation of the pH-dependent kinetic data. Thus, the probes that detect nucleophilic reactivity in Cys25 at low pH (**1** and **4**) react with papain via quasi-transition states in which the protonated pyridyl ring is remote from Trp177 (panels D and C of Figure 7, respectively). In marked contrast, those that fail to detect nucleophilic reactivity in Cys25 at low pH (**2** and **3**) react via quasi-transition states in which the protonated pyridyl ring is bound in the proximity of the indole ring system of Trp177 (panels A and B of Figure 7, respectively). The fact that the minimum energy conformations show the planes of the rings to be almost perpendicular to each other suggests that cation−π interaction (*34*) does not contribute significantly to the binding. Rather, the impedance to the movement of Trp177 required to decrease the level of mutual solvation of the components of the (Cys25)−S^-/(His159)−Im^+H ion pair results from an increase in the packing density in that region. The indole ring system is packed against the pyridyl ring which in turn is packed against the wall of the cleft.

It is important to point out that the amino probe with trimethylene spacer **3**, one of the probes that does not detect nucleophilic reactivity in Cys25, is bound remotely from the carboxylate side chain of Asp158 and does not perturb its interactions with the papain chain. Thus, it is the interactions of probes **2** and **3** with Trp177 that correlate with loss of nucleophilic character in Cys25 and not interaction with (Asp158)−CO_2^-.

It has been appreciated for a long time that the Cys25 and His159 components of the catalytic site ion pair, being on opposite sides of the active center cleft of papain, are susceptible to movement consequent to ligand binding in the cleft (*35*). In this work, the motions of the cleft around Trp177 were compared in the quasi-transition states for the reactions of papain with probes **2** and **4**. The latter detects nucleophilic character in Cys25 at low pH, whereas the former does not. Normal mode analysis is used to approximate overall motion in a molecule in terms of its vibrational components (*29*) (see, e.g., ref *36*). In the quasi-transition state of the reaction with probe **2**, described in the Results, the mutual solvation of (Cys25)−S^- and (His159)−Im^+H is maintained because the movement of Trp177 is contained within the symmetrically moving walls of the cleft. In the reaction of probe **4**, however, the motion of the cleft is antisymmetric around the Trp177 region which results in His159 being exposed to solvent with a consequent decrease in its level of solvation of (Cys25)−S^-. This perturbation of the solvation of the (Cys25)−S^-/(His159)−Im^+H ion pair is predicted to release nucleophilic character in Cys25. It is suggested, therefore, that it is the decrease in the extent of hydrophobic shielding of the Cys25/His159 ion pair by the movement of the cleft around the Trp177 region that promotes the generation of nucleophilic character in the ion pair as the initial mechanistic event in catalysis by papain.

REFERENCES

1. Barrett, A. J., Rawlings, N. D., and Woessner, J. F., Jr., Eds. (2004) *Handbook of proteolytic enzymes*, Elsevier, London.
2. Brocklehurst, K., Willenbrock, F., and Salih, E. (1987) Cysteine proteinases, in *Hydrolytic Enzymes: New Comprehensive Bio-*

chemistry (Neuberger, A., and Brocklehurst, K., Eds.) Vol. 16, pp 39−158, Elsevier, Amsterdam.
3. Brocklehurst, K., Watts, A. B., Patel, M., Verma, C. S., and Thomas, E. W. (1998) Cysteine proteinases, in *Comprehensive Biological Catalysis* (Sinnot, M. L., Ed.) Vol. 1, pp 381−423, Academic Press, London.
4. Hussain, S., Khan, A., and Brocklehurst, K. (2002) A review of developments in the study of cysteine proteinase mechanism: Opportunities for the investigation of electrostatic effects and dynamic aspects of molecular recognition in enzyme chemistry, *Recent Res. Dev. Biochem. 3*, 653−677.
5. Gul, S., Mellor, G. W., Thomas, E., and Brocklehurst, K. (2006) Temperature-dependences of the kinetics of reactions of papain and actinidin with a series of reactivity probes differing in key molecular recognition features, *Biochem. J. 396*, 17−21.
6. O'Farrell, P. A., and Joshua-Tor, L. (2007) Mutagenesis and crystallographic studies of the catalytic residues of the papain family protease bleomycin hydrolase: New insights into active-site structure, *Biochem. J. 401*, 421−428.
7. Jackson, S. E., and Fersht, A. R. (1993) Contribution of long-range electrostatic interactions to the stabilization of the catalytic transition state of the serine protease subtilisin BPN′, *Biochemistry 32*, 13909−13916.
8. Plou, F. J., Kowlessur, D., Malthouse, J. P., Mellor, G. W., Hartshorn, M. J., Pinitglang, S., Patel, H., Topham, C. M., Thomas, E. W., Verma, C., and Brocklehurst, K. (1996) Characterization of the electrostatic perturbation of a catalytic site (Cys)−S^-/(His)−Im^+H ion-pair in one type of serine proteinase architecture by kinetic and computational studies on chemically mutated subtilisin variants, *J. Mol. Biol. 257*, 1088−1111.
9. Duncan, G. D., Huber, C. P., and Welsh, W. J. (1992) Molecular orbital studies of the structure and reactivity of model substrate intermediates in the deacylation of the cysteine protease papain, *J. Am. Chem. Soc. 114*, 5784−5794.
10. Pickersgill, R. W., Sumner, I. G., Collins, M. E., and Goodenough, P. W. (1989) Structural and electrostatic differences between actinidin and papain account for differences in activity, *Biochem. J. 257*, 310−312.
11. Kowlessur, D., O'Driscoll, M., Topham, C. M., Templeton, W., Thomas, E. W., and Brocklehurst, K. (1989) The interplay of electrostatic fields and binding interactions determining catalytic site reactivity in actinidin. A possible origin of differences in the behaviour of actinidin and papain, *Biochem. J. 259*, 443−452.
12. Ménard, R., Khouri, H. E., Plouffe, C., Dupras, R., Ripoll, D., Vernet, T., Tessier, D. C., Lalberte, F., Thomas, D. Y., and Storer, A. C. (1990) A protein engineering study of the role of aspartate 158 in the catalytic mechanism of papain, *Biochemistry 29*, 6706−6713.
13. Taylor, M. A. J., Baker, K. C., Connerton, I. F., Cummings, N. J., Harris, G. W., Henderson, I. M., Jones, S. T., Pickersgill, R. W., Sumner, I. G., Warwicker, J., and Goodenough, P. W. (1994) An unequivocal example of cysteine proteinase activity affected by multiple electrostatic interactions, *Protein Eng. 10*, 1267−1276.
14. Guarné, A., Hampoelz, B., Glaser, W., Carpena, X., Tormo, J., Fita, I., and Skern, T. (2000) Structural and biochemical features distinguish the foot-and-mouth disease virus leader proteinase from other papain-like enzymes, *J. Mol. Biol. 302*, 1227−1240.
15. Schlick, P., Kronovetr, J., Hampoelz, B., and Skern, T. (2002) Modulation of the electrostatic charge at the active site of foot-and-mouth-disease-virus leader proteinase, an unusual papain-like enzyme, *Biochem. J. 363*, 493−501.
16. Carter, C. E., Marriage, H., and Goodenough, P. W. (2000) Mutagenesis and kinetic studies of a plant cysteine proteinase with an unusual arrangement of acidic amino acids in and around the active site, *Biochemistry 39*, 11005−11013.
17. Hussain, S., Pinitglang, S., Bailey, T. S., Reid, J. D., Noble, M. A., Resmini, M., Thomas, E. W., Greaves, R. B., Verma, C. S., and Brocklehurst, K. (2003) Variation in the pH-dependent pre-steady-state and steady-state kinetic characteristics of cysteine-proteinase mechanism: Evidence for electrostatic modulation of catalytic site function by the neighbouring carboxylate anion, *Biochem. J. 372*, 735−746.
18. Pinitglang, S., Watts, A. B., Patel, M., Reid, J. D., Noble, M. A., Gul, S., Bokth, A., Naeem, A., Patel, H., Thomas, E. W., Sreedharan, S. K., Verma, C., and Brocklehurst, K. (1997) A classical enzyme active center motif lacks catalytic competence until modulated electrostatically, *Biochemistry 36*, 9968−9982.
19. Noble, M. A., Gul, S., Verma, C. S., and Brocklehurst K. (2000) Ionization characteristics and chemical influences of aspartic acid residue 158 of papain and caricain determined by structure-related kinetic and computational techniques: Multiple electrostatic modulators of active-centre chemistry, *Biochem. J. 351*, 723−733.
20. Baines, B. S., and Brocklehurst, K. (1979) A necessary modification to the preparation of papain from any high-quality latex of *Carica papaya* and evidence for the structural integrity of the enzyme produced by traditional methods, *Biochem. J. 177*, 541−548.
21. Brocklehurst, K., Courey, A. J., Gul, S., Lin, S., and Moritz, R. L. (2004) Affinity and immunoaffinity chromatography, in *Purifying Proteins for Proteomics: A Laboratory Manual* (Simpson, R. J., Ed.) pp 221−273, Cold Spring Harbor Laboratory Press, Plainview, NY.
22. Baines, B. S., and Brocklehurst, K. (1978) A spectrophotometric method for the detection of contaminant chymopapains in preparations of papain: Selective modification of one type of thiol group in the chymopapains by a two-protonic-state reagent, *Biochem. J. 173*, 345−347.
23. Shipton, M., and Brochlehurst, K. (1978) Characterization of the papain active centre by using two-protonic-state electrophiles as reactivity probes. Evidence for nucleophilic reactivity in the uninterrupted cysteine-25-histidine-159 interactive system, *Biochem. J. 171*, 385−401.
24. Stuchbury, T., Shipton, M., Norris, R., Malthouse, J. P., Brocklehurst, K., Herbert, J. A., and Suschitzky, H. (1975) A reporter group delivery system with both absolute and selective specificity for thiol groups and an improved fluorescent probe containing the 7-nitrobenzo-2-oxa-1,3-diazole moiety, *Biochem. J. 151*, 417−432.
25. Dirscherl, W., and Weingarten, S. W. (1951) Synthese von homologen des cystamins, *Annalen 574*, 131−139.
26. Kamphius, I. G., Kalk, K. H., Swarte, M. B. A., and Drenth, J. (1984) Structure of papain refined at 1.6 Å resolution, *J. Mol. Biol. 179*, 233−256.
27. Cohen, L. W., Coghlan, V. M., and Dihel, L. C. (1986) Cloning and sequencing of papain-encoding cDNA, *Gene 48*, 219−227.
28. Brunger, A. T., and Karplus, M. (1988) Polar hydrogen positions in proteins: Empirical energy placement and neutron diffraction comparison, *Proteins 4*, 148−156.
29. Berendsen, H. J. C., and Hayward, S. (2000) Collective protein dynamics in relation to function, *Curr. Opin. Struct. Biol. 10*, 165−169.
30. Brocklehurst, K. (1994) A sound basis for pH-dependent kinetic studies in enzymes, *Protein Eng. 7*, 291−299.
31. Brocklehurst, K. (1979) The equilibrium assumption is valid for the kinetic treatment of most time-dependent protein modification reactions, *Biochem. J. 181*, 775−778.
32. Brocklehurst, S. M., Topham, C. M., and Brocklehurst, K. (1990) A general kinetic equation for multihydronic state reactions and rapid procedures for parameter evaluation, *Biochem. Soc. Trans. 18*, 598−599.
33. Brocklehurst, K. (1982) Two-protonic-state electrophiles as probes of enzyme mechanism, *Methods Enzymol. 87C*, 427−469.
34. Ma, J. C., and Dougherty, D. A. (1997) The cation-π interaction, *Chem. Rev. 97*, 1303−1324.
35. Drenth, J., Kalk, K. H., and Swen, H. M. (1976) Binding of chloromethyl ketone substrate analogues to crystalline papain, *Biochemistry 15*, 3731−3738.
36. Miller, D. W., and Agard, D. A. (1999) Enzyme specificity under dynamic control: A normal mode analysis of α-lytic protease, *J. Mol. Biol. 286*, 267−278.
37. DeLano, W. L. (2000) *The PyMOL Molecular Graphics System*, DeLano Scientific, San Carlos, CA.

BI702126P